Appl Phys B (2011) 103: 405–411
DOI 10.1007/s00340-010-4309-y

Applied Physics B
Lasers and Optics

Propagation of low-intensity Gaussian fields in photorefractive media with real and imaginary intensity-dependent refractive index components

M.W. Jones · E. Jaatinen · G.W. Michael

Received: 23 June 2010 / Revised version: 11 October 2010 / Published online: 23 November 2010

Abstract A theoretical analysis of a low power Gaussian field propagating in unbiased self-defocussing photorefractive media that includes both real and imaginary components of the intensity-dependent refractive index is presented. The analysis, which is in excellent agreement with experimental observations, shows that the imaginary component of the intensity-dependent refractive index can have a focussing effect independent of the focussing or defocussing effect of the real component of the intensity-dependent refractive index. These findings suggest that the imaginary component of the intensity-dependent refractive index is the cause of the previously observed apparent self-focussing in unbiased self-defocussing photorefractive media.

1 Introduction

One of the current challenges facing both the communications and computing industries is the need to increase information capacity and processing speed. Optical devices, which use light to control light, have long been touted as one possible solution, offering vast improvements in capacity and speed, as well as offering the possibility to be completely reconfigurable when created in photosensitive media [1–3]. Analogous to electronic circuitry, the functionality and operating speed of such devices would increase if the size of the device was reduced, which requires minimising the divergence of each beam over the distance it travels [4–6]. Ideally, these low-divergence fields will operate at low powers where current communications technology exists [7] allowing easy integration and ensuring lower power consumption, low heat generation, and few safety concerns. Future optical devices used for optical communications and switching will most likely use compact semiconductor lasers, with Gaussian intensity profile outputs, and therefore, a complete understanding of the effect of photosensitive media on the propagation of low optical power Gaussian beams is imperative.

Recently, photorefractive self-focussing was observed in both doped and undoped unbiased self-defocussing $BaTiO_3$ where the photorefractive (PR) media was placed at the beam waist position of a tightly focused TEM_{00} Gaussian field [8]. Following this, the conditions where low power TEM_{00} Gaussian fields can propagate in self-defocussing PR media without divergence while maintaining their Gaussian spatial profile were theoretically identified in terms of both real and imaginary components of the refractive index [9]. This theoretical model used the findings that a low optical power beam with a Gaussian spatial intensity profile incident on Ce:$BaTiO_3$ maintains its Gaussian profile as it propagates through the medium [9] and that under these conditions, the refractive index profile of the medium can be approximated as quadratic [10].

In this paper the low-intensity conditions where the PR medium can be approximated as having a quadratic refractive index profile and where the beam can be described by a Gaussian spatial profile are examined. In particular, the threshold intensity for where the low-intensity quadratic approximation is valid is considered. Under these conditions, the effect of the imaginary component of the intensity-dependent refractive index on the propagation of the Gaussian beam is investigated. The important role that the imaginary component plays in overall medium behav-

M.W. Jones (✉) · E. Jaatinen · G.W. Michael
Applied Optics and Nanotechnology, Faculty of Science and Technology, Queensland University of Technology, 2 George Street, Brisbane, 4000, Australia
e-mail: mw.jones@qut.edu.au
Fax: +61-7-31389079

iour is demonstrated by the excellent agreement between the theoretical treatment and the presented experimental observations. In particular, it will be shown that the apparent self-focussing observed in a nominally self-defocussing PR crystal [8] can be explained with the inclusion of this refractive index component.

2 Theory

It is well known that in a PR material that the refractive index is dependent on the intensity of the light travelling through it [11, 12]. At high intensities the refractive index depends nonlinearly on the intensity of the incident field, however, at low intensities ($I \approx \mathrm{mW\,mm^{-2}}$) the dependence can be approximated as the first term in the Taylor expansion [13]. For TEM_{00} Gaussian incident fields at these low intensities, the variation of the wavevector, k, with the transverse distance from the beam axis, r, can be treated as quadratic and is given by [14];

$$k^2(r) = k_0^2 n_0^2 - k_0 n_0 k_2 r^2 \tag{1}$$

Here k_0 is the wavevector in a vacuum, n_0 is the background refractive index, k_2 contains the intensity-dependent refractive index change:

$$k_2 = \frac{4 n_2 I_0 k_0}{w^2(z)} \tag{2}$$

where n_2 is the intensity-dependent refractive index coefficient, I_0 is the intensity on the beam axis, and $w(z)$ is the radius of the beam. However, the intensity-dependent refractive index of most PR materials possesses both real and imaginary terms [9]:

$$k^2(r) = k_0^2 n_0^2 - k_0 n_0 k_{2R} r^2 - i k_0 n_0 k_{2I} r^2 \tag{3}$$

Conceptually, the real part of the intensity-dependent wavevector (k_{2R}), gives the intensity-dependent refractive index change of the medium, while the imaginary part (k_{2I}) gives the intensity-dependent absorption or transparency:

$$k_{2R} = \frac{4 n_{2R} I_0 k_0}{w^2(z)}, \tag{4a}$$

$$k_{2I} = \frac{4 n_{2I} I_0 k_0}{w^2(z)} \tag{4b}$$

PR materials can have $k_{2R} > 0$ or $k_{2R} < 0$, corresponding to media that is nominally self-focussing or self-defocussing respectively. Here, self-focussing and self-defocussing refer to the decrease or increase in the Gaussian beam diameter as a result of the photo-induced change in refractive index due to the well-known χ_3 nonlinearity of $BaTiO_3$. Additionally, materials with $k_{2I} > 0$ display an increase in transparency as the field intensity increases, while those with $k_{2I} < 0$ display increased absorption. It has been shown that a specific PR material can show either intensity-dependent absorption or transparency depending on the incident wavelength [15–17] providing a means to practically dictate the sign of k_{2I}.

A Gaussian field propagating within this quadratic medium can be expressed as [14]:

$$E(r, z) = \psi(r, z) \exp(-ikz), \tag{5a}$$

$$\psi(r, z) = \exp[-iP(z)] \exp\left[-i \frac{Q(z) r^2}{2}\right] \tag{5b}$$

where $Q(z)$ gives the transverse variation of field amplitude and phase while $P(z)$ gives the amplitude variation due to the beam's convergence or divergence. The Gaussian beam amplitude can be rewritten as

$$E(r, z) = \sqrt{\frac{P_0}{\pi w^2(z)}} \exp[-i\theta(z)] \times \exp[-ik(z)] \exp\left[-i \frac{r^2 k}{q(z)}\right], \tag{6a}$$

$$Q(z) = \frac{k}{q(z)} = \frac{k}{R(z)} - i \frac{2}{w^2(z)}, \tag{6b}$$

$$P(z) = \theta(z) + i \ln\left[\sqrt{\frac{P(0)}{\pi w^2(z)}}\right] \tag{6c}$$

Here $w(z)$ and $R(z)$ are the well-known functions describing the variation of the beam radius and wavefront curvature as the field propagates in the z direction.

Upon substitution into the wave equation

$$\nabla^2 E + \left(k^2 - k k_2 r^2\right) E = 0 \tag{7}$$

We obtain

$$Q^2 + k Q' + k k_{2R} + i k k_{2I} = 0, \tag{8a}$$

$$P' = \frac{-i Q}{k} \tag{8b}$$

These can be solved, yielding

$$Q(z) = \sqrt{k}\sqrt{k_{2R} + i k_{2I}} \times \tan\left[-\frac{\sqrt{k_{2R} + i k_{2I}}}{\sqrt{k}} z + D_R + i D_I\right] \tag{9}$$

Here D_R and D_I are real constants of integration. The trigonometric function can be separated into real and imaginary parts, using:

$$a + ib = \sqrt{k_{2R} + i k_{2I}},$$

$$k_{2R} = a^2 - b^2,$$

$$k_{2I} = 2ab, \tag{10}$$
$$2a^2 = k_{2R} + \sqrt{k_{2R}^2 + k_{2I}^2},$$
$$2b^2 = -k_{2R} + \sqrt{k_{2R}^2 + k_{2I}^2}$$

Substituting (10) into (9) and applying trigonometric identities we get

$$Q(z) = -\sqrt{k}(a+ib)\tan\left[\frac{a}{\sqrt{k}}z - D_R + i\left(\frac{b}{\sqrt{k}}z - iD_I\right)\right]$$
$$= -\sqrt{k}\left\{\begin{array}{l}\frac{a\sin\left[2\frac{a}{\sqrt{k}}z+C1\right]-b\sinh\left[2\frac{b}{\sqrt{k}}z+C2\right]}{\cos\left[2\frac{a}{\sqrt{k}}z+C1\right]+\cosh[2\frac{b}{\sqrt{k}}z+C2]} \\ +i\frac{a\sinh\left[2\frac{b}{\sqrt{k}}z+C2\right]+b\sin\left[2\frac{a}{\sqrt{k}}z+C1\right]}{\cos\left[2\frac{a}{\sqrt{k}}z+C1\right]+\cosh[2\frac{b}{\sqrt{k}}z+C2]}\end{array}\right\} \tag{11}$$

Equating this with (6b) gives the wavefront curvature and beam radius as a function of distance through the medium.

$$R(z) = -\sqrt{k}\frac{\cos\left[2\frac{a}{\sqrt{k}}z+C1\right]+\cosh\left[2\frac{b}{\sqrt{k}}z+C2\right]}{a\sin\left[2\frac{a}{\sqrt{k}}z+C1\right]-b\sinh\left[2\frac{b}{\sqrt{k}}z+C2\right]}, \tag{12a}$$

$$w^2(z) = \frac{2}{\sqrt{k}}\frac{\cos\left[2\frac{a}{\sqrt{k}}z+C1\right]+\cosh\left[2\frac{b}{\sqrt{k}}z+C2\right]}{b\sin\left[2\frac{a}{\sqrt{k}}z+C1\right]+a\sinh\left[2\frac{b}{\sqrt{k}}z+C2\right]} \tag{12b}$$

The two integration constants $C1$ and $C2$ are then evaluated using the boundary conditions for beam radius and wavefront curvature. This is made easier by noting the relationship:

$$\frac{w^2(z=0)}{R(z=0)} = \frac{w_i^2}{R_i} = \frac{2}{k}\frac{2z_0}{kw_0^2}$$
$$= \frac{2}{k}\frac{b\sinh(C2)-a\sin(C1)}{b\sin(C1)+a\sinh(C2)} \tag{13}$$

Equations (10), (11), and (12) apply to focussing media ($|a| < |b|$), defocussing media ($|a| > |b|$), and media with an intensity-dependent absorption ($ab > 0$) or intensity-dependent transparency ($ab < 0$). From here, a variety of scenarios can be described where the incident intensity is independent of the propagation distance.

For example, a beam will propagate in PR media without spatial divergence when the beam radius and wavefront curvature are independent of the propagation distance, z. In self-focussing PR media, beams propagating without spatial divergence known as spatial solitons are formed when the wavefronts have infinite curvature ($R \to \infty, z = 0$). Under these conditions, (12b) reduces to

$$w^2 = \frac{2}{\sqrt{k_{2R}k}} \tag{14}$$

Note for (12a) to be satisfied, $k_{2I} = 0$ which implies that for a soliton of this type to form the medium should display no intensity-dependent absorption. In terms of the required change in refractive index, n_{2R}, using (2), (14) displays a similar dependence to beam area and intensity as the well-known solution of spatial soliton propagating with a sech profile [18, 19]:

$$n_{2R} = \frac{\lambda^2}{4\pi^2 I_0 w^2 n_0} \tag{15}$$

For a Gaussian beam to propagate without divergence in self-defocussing PR media, (12a) and (12b) become

$$R(z) = R_i = \frac{\sqrt{k}}{b}, \tag{16a}$$

$$w^2(z) = w_i^2 = \frac{2}{a\sqrt{k}} \tag{16b}$$

Under the appropriate boundary conditions, the values of k_{2R} and k_{2I} required for this to occur are determined from (12) and (14) and are in good agreement with previous research [9]:

$$k_{2R} = a^2 - b^2 = \frac{4}{kw_i^4} - \frac{k}{R_i^2}, \tag{17a}$$

$$k_{2I} = 2ab = \frac{4}{w_i^2 R_i} \tag{17b}$$

2.1 Numerical model

The analytical treatment of self-focussing and self-defocussing PR media described in the previous section is only valid when the field intensity does not vary as the beam propagates through the medium. In many practical applications however, this is not the case, and it follows that the real and imaginary parts of the refractive index will also be functions of propagation distance. Therefore, to incorporate these intensity variations, the propagation of Gaussian beams in PR media with a quadratic refractive index change [9] was numerically modelled.

Under low-intensity illumination, a beam with a Gaussian spatial intensity distribution will maintain its spatial intensity distribution as it propagates through a PR medium [9]. This significantly simplifies the numerical process since by forcing the transverse field distribution to be of the known TEM_{00} Gaussian, the wave equation is reduced to a first order differential equation [20].

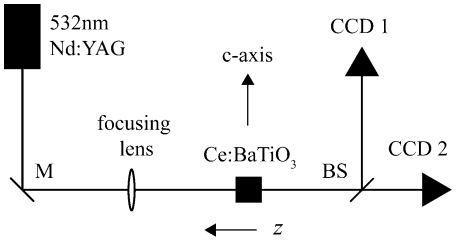

Fig. 1 Experimental arrangement used to measure the far-field profile of the Gaussian beam at two different propagation distances with two CCD cameras (*CCD1* and *CCD2*), a flat mirror (*M*), and a 50/50 beam splitter (*BS*). The crystal was translated in the z direction, as indicated by the *arrow*, with the optical c-axis orthogonal to the direction of propagation

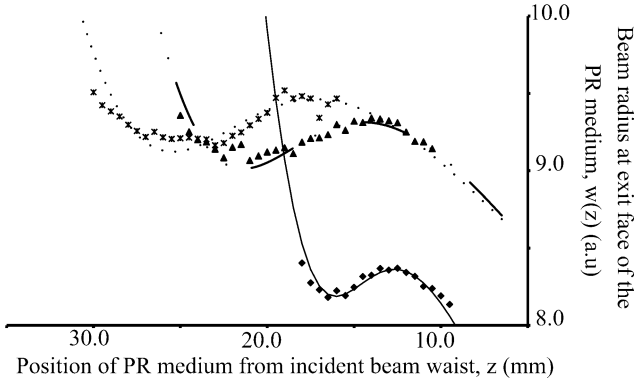

Fig. 2 Numerical and experimental results of the effect of change in beam power and waist size. The *crosses* and *triangles* represent experimental results from an incident beam with an initial beam waist, $w(0)$ of 35 μm at powers of 1.2 mW and 1.4 mW respectively. The *dotted line* and the *dashed line* depict the theoretical results for each case respectively. The *diamonds* represent experimental results for an incident beam with a waist of 25 μm and beam power of 1.2 mW, with the *solid line* representing the theoretical plot for this case

3 Experimental investigation

$Ce:BaTiO_3$ is a self-defocussing PR material that displays intensity-dependent absorption at 532 nm. Since both the PR medium and wavelength are widely used, they were selected to investigate the predictions of the theoretical approach outlined previously. The experimental layout was essentially a z-scan arrangement as shown in Fig. 1. A converging TEM_{00} Gaussian beam from a horizontally polarised, frequency doubled Nd:YAG laser operating at 532 nm with a beam power less than 4 mW was incident on an unbiased $Ce:BaTiO_3$ self-defocussing photorefractive crystal. The crystal had a Cerium concentration of 50 ppm, and dimensions of 5 mm × 5 mm × 5 mm. The optical c-axis of the crystal was orientated in the horizontal plane, perpendicular to the direction of beam propagation, as indicated in Fig. 1. The PR crystal was placed at a distance greater than the Rayleigh length ($z_R = \pi w_0^2/\lambda$) in front of the beam waist position, and translated with respect to the beam waist in a direction parallel to the beam propagation direction in 0.5 mm increments.

After propagating through the PR crystal, a 50/50 beam splitter was used to obtain two images of the far field at two distances with a separation of 95 mm, allowing the beam divergence, and hence the beam waist and position to be calculated. The far field at each of the two different positions was imaged with two CCD cameras, with the images then analysed by least squares fitting 40 Gaussian profiles to the 40 pixel rows centred on the maximum intensity of the intensity profile of the image. The average of these Gaussian profiles was determined, yielding a value for the diameter of the Gaussian beam, defined as the distance from the beam axis where the intensity fell to e^{-2} of its peak value, together with an estimate of the uncertainty in the diameter. The measurement was repeated four times at each z position, and the average of the results was taken. The experimental configuration is shown in Fig. 1.

The diameter of the Gaussian beam at the two far-field positions allowed the far-field divergence angle and the position of the beam waist after propagating through the PR crystal (w_2) to be determined using the well-known relationship:

$$\theta = \frac{\lambda}{\pi w_2} \tag{18}$$

The radius of the beam at the exit face of the PR crystal is then calculated using w_2 and the distance from the waist to the exit face.

To confirm theoretical model predictions relating to the dependence on the beam waist size and beam power of the incident beam, experimental measurements were performed for incident beams with waists of 35 μm and 25 μm and with incident optical beam powers of 1.2 mW and 1.4 mW. This range of experimental conditions was sufficient to produce significantly different results, without violating the quadratic approximation for the refractive index variation (i.e. (1)). Under these experimental conditions, the contribution of thermally induced changes to the refractive index are negligible [21].

Figure 2 shows the dependence of the beam radius at the exit face of the medium on incident beam intensity. Here the incident intensity is varied by shifting the location of the medium with respect to the initial beam waist position, varying the incident optical beam power, or by changing the size of the initial beam waist. The results predicted by the numerical model are in excellent agreement with the observations demonstrating its validity and accuracy. The only adjustable parameters used in the model are $n_{2R}I_0$ and $n_{2I}I_0$ which were both estimated from measurements [9] to be in the order of -10^{-6} and 10^{-7} respectively.

As Fig. 2 demonstrates, significant variation in behaviour can occur with subtle changes in experimental conditions. Similar agreement between the theoretical treatment and experimental observations was found under other conditions in

the low optical power regime (<4 mW). In all cases, the observed features could only be explained by the model with the inclusion of the imaginary component of the intensity-dependent refractive index. The importance of this component in explaining self-focussing and self-defocussing behaviour will be discussed in a later section of this paper.

4 Quadratic refractive index profile approximation

A well-known medium with a quadratic refractive index profile is a Graded Index (GRIN) lens. These focussing optics have a refractive index variation given by [22]:

$$n(r) = n_0\left(1 - \frac{A}{2}r^2\right) \tag{19}$$

Therefore, assuming the PR media has a refractive index profile that can be approximated as being quadratic, and that the Gaussian spatial profile of the incident beam is preserved, self-focussing and self-defocussing PR media should act analogously to an intensity-dependent GRIN lenses with positive and negative focal lengths respectively, given by [10]:

$$f_{f,d} \approx \frac{1}{n_0 d A} = \frac{\pm w^2}{4|n_2|I_0 d} \tag{20}$$

To determine the range over which the PR medium can be approximated as having a quadratic refractive index profile, the analytical solution given in (20), numerical results allowing both the real and imaginary parts of the refractive index to be functions of propagation distance, and experimental data were compared. Where the numerical and experimental results diverge indicates at the limiting intensity at which the low-intensity regime is no longer applicable and the medium can no longer be described as having a quadratic refractive index profile.

The effective focal length for a 5 mm long self-defocussing Ce:$BaTiO_3$ PR crystal with an incident beam waist of 35 μm was calculated using incident and exit values for $w(z)$ and $R(z)$ together with Gaussian beam transformation formulae for a thick lens. These beam parameters at the incident and exit faces of the medium were calculated numerically allowing for the change in refractive index to include both real and imaginary components. In the numerical model, the same values for n_{2R} and n_{2I} were used as in the previous section. The z-scan experimental technique was used to vary the beam intensity of a TEM_{00} Gaussian incident beam at a wavelength of 532 nm with a beam waist of 35 μm and incident optical beam powers of 0.6 mW and 1.2 mW.

When the incident intensity is low, the experimental results show good agreement with the analytical approximation given by (20), and with the numerical results that include the imaginary component of the change in refractive index. In this region of low intensity, the excellent agreement shows that the PR medium can be approximated as having a quadratic change in refractive index. As the intensity increases, numerical and experimental results deviate sharply from the analytical approximation. At this point, the numerical and experimental results continue to show good agreement, illustrating the significant impact that the imaginary component of the refractive index has on the Gaussian beam propagation in this intensity range. This trend continues up to an incident intensity of approximately 2.0 W mm^{-2}, where the experimental and numerical results diverge. Therefore, at greater intensities the medium can no longer be approximated as having a quadratic refractive index profile, and the numerical model can no longer be considered valid.

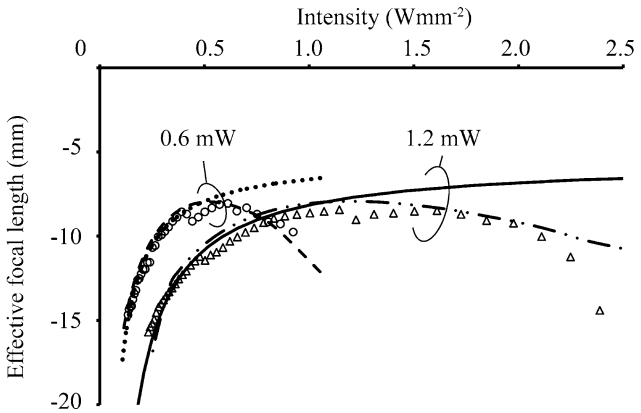

Fig. 3 Focal length of the PR medium as a function of incident intensity. The figure shows analytical results from (20) (*dotted* and *solid line*), numerical results including k_{2I} (*dashed* and *dash-dot line*), and experimental results (*circles* and *triangles*) for incident optical beam powers of 0.6 mW and 1.2 mW respectively

5 The imaginary component of the refractive index

In the previous sections it was found that both the real and imaginary parts of the intensity-dependent refractive index must be included in the theoretical treatment in order to accurately describe experimental observations. At low incident intensities (less than 20 mW mm^{-2}), the propagation of a Gaussian beam through a PR medium was numerically modelled. To highlight the effect of the imaginary component of the refractive index on the beam propagation, self-focussing and self-defocussing PR media with positive and negative imaginary components of the change in refractive index were theoretically analysed with both incident converging and diverging beams. The results are presented in Fig. 4, which shows beam radius as a function of propagation distance through the medium placed one metre from the beam waist ($w_0 = 25$ μm) with a wavelength of 532 nm. In

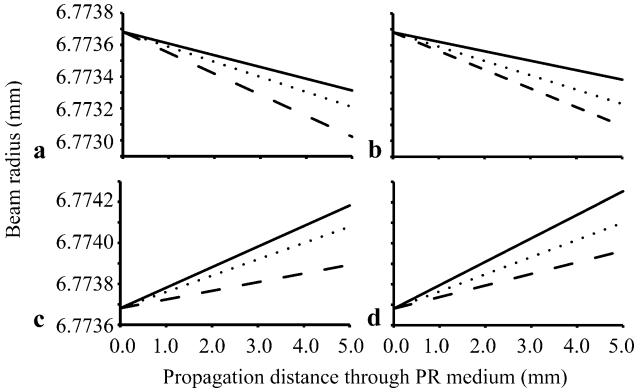

Fig. 4 Beam radius as a function of propagation distance through a PR medium placed one metre from the beam waist with k_{2I} positive (*dashed lines*) and negative (*solid lines*) for converging ($z = -1$ m) incident Gaussian beams in self-focussing (**a**) and self-defocussing (**b**) PR media, and diverging ($z = +1$ m) incident Gaussian beams in self-focussing (**c**) and self-defocussing (**d**) PR media. In all cases, the dotted line represents the propagation of the Gaussian beam in the absence of k_{2I}

this case the magnitudes of $n_{2R}I_0$ and $n_{2I}I_0$ are equal to 2×10^{-8} and 2×10^{-10} respectively.

These results clearly show that in all cases, when k_{2I} is negative the beam radius increases, while where k_{2I} is positive the beam radius decreases relative to the case where k_{2I} is equal to zero. It is also evident that this effect occurs independently, and in addition to the self-focussing or defocussing nature of the medium, and it is independent of the initial convergence or divergence of the incident beam. Therefore, the nonlinear absorption, k_{2I}, can lead to 'apparent' focussing and defocussing effects independent of k_{2R}. When $k_{2I} > 0$, the intensity-dependent absorption is strongest at the centre of the Gaussian beam, where the intensity is the highest, while in the wings of the beam the absorption is weaker. Consequently, a greater reduction in intensity occurs on beam axis than in the wings producing a broader beam as measured at the e^{-2} intensity points. The converse applies when $k_{2i} < 0$. In Ce:$BaTiO_3$, for example, k_{2I} is positive and k_{2R} is negative at incident wavelengths of 532 nm and 633 nm [17], leading to the possibility of apparent self-focussing in a self-defocussing PR medium.

6 Self-focussing in self-defocussing PR media

Self-defocussing PR media has an intensity-dependent change in refractive index that causes a Gaussian beam to diverge as it propagates through the media. Thus, if a Gaussian field is arranged such that the beam waist falls on the entrance face of a self-defocussing PR medium, then the expectation is that the diameter of the beam that emerges from the medium will be larger than what would be observed if the medium had no PR properties. Recently however, it was found that this was not always the case, with anomalous self-focussing effects observed in self-defocussing $BaTiO_3$ [8] at a wavelength of 633 nm, where intensity-dependent absorption ($k_{2I} > 0$) is observed [17, 23]. In that work the authors observed that when an undoped self-defocussing PR material is placed at the beam waist of a tightly focused beam with an intensity of 2×10^{-3} W mm^{-2}, the radius of the beam that exits the 5 mm thick medium, reduces to 70% of the initial exit beam size after approximately 1000 seconds. In the following treatment it will be shown that one possible explanation for these anomalous observations is the focussing effects due to the imaginary part of the intensity-dependent refractive index discussed in the previous section. Assuming that the medium is not too thick, $t \leq z_R$, the variation of the peak intensity of the beam propagating from the beam waist over the extent of the medium's length can be ignored, and k_{2R} and k_{2I} can be treated as constants. Using the boundary conditions given in (13) for the situation where a self-defocussing PR medium is placed at the beam waist and $k_{2R} < 0$ and $k_{2I} > 0$, the constants in (12a) and (12b) are

$$
\begin{aligned}
a &= \sqrt{\frac{k_{2R} + \sqrt{k_{2R}^2 + k_{2I}^2}}{2}}, \\
b &= -\sqrt{\frac{-k_{2R} + \sqrt{k_{2R}^2 + k_{2I}^2}}{2}}, \\
C1 &= \sin^{-1}\left[\frac{b}{a}\sinh(C2)\right], \\
C2 &= \tanh^{-1}\left(\frac{w_i^2\sqrt{k}b^2}{w_i^2\sqrt{k}b^2 a + \frac{2b^2}{a} + 2a}\right)
\end{aligned}
\tag{21}
$$

Using values for the intensity-dependent refractive indices, $n_{2R}I_0$ and $n_{2I}I_0$, of -2×10^{-6} and 3×10^{-8} respectively, the beam radius as the beam propagates through the PR medium can be calculated. These values for the change in refractive indices were derived from reported values for the intensity-dependent refractive index change and intensity-dependent absorption in $BaTiO_3$ at 633 nm [17, 24, 25]. The results are shown in Fig. 5 (dotted line), and show that according to the analytical model, a beam with a radius of 4 μm located at the entrance face of the self-defocussing PR medium exits with a radius slightly larger than it would if the medium had a homogeneous refractive index (solid line). With a thickness of 5 mm, the PR medium is significantly thicker than the Rayleigh length, $t > z_R \approx 0.2$ mm, and the assumption that k_{2R} and k_{2I} are constant is not valid. However, for propagation distances less than z_R, the analytical approach results show an apparent self-focussing when compared to the homogeneous case, before defocussing as expected. The initial propagation distances are expanded in

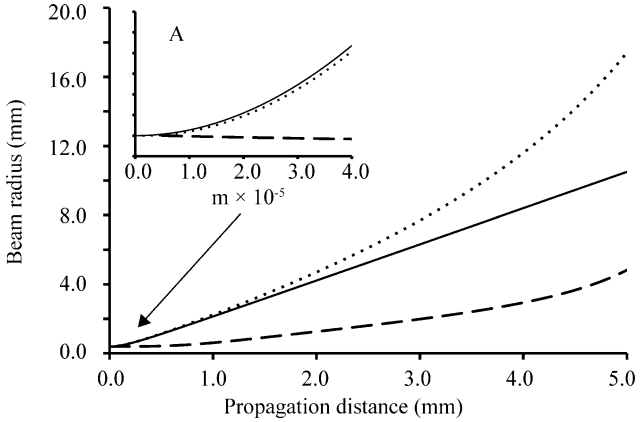

Fig. 5 Beam radius as a function of propagation distance through a self-defocussing PR medium when the beam waist is placed at the entrance face of a self-defocussing PR medium. Shown are the case for a homogeneous media (*solid line*), the analytical analysis (*dotted line*), and the numerical consideration (*dashed line*)

insert A, Fig. 5. To examine longer propagation distances, the change in the real and imaginary parts of the change in refractive index as functions of the propagation distance were considered numerically. The results of the numerical model are presented in Fig. 5 (dashed line) and show the beam exiting the PR crystal with a beam radius of approximately 50% of the size of the homogeneous case, apparently self-focussing, as previously observed [8].

7 Conclusion

A theoretical analysis is presented that includes both the real and imaginary parts of the intensity-dependent refractive index that agrees well with observations of low-intensity TEM_{00} Gaussian beams propagating through photorefractive media. In this model the medium is treated as having a quadratically varying refractive index profile that ensures that the field propagating through it, retains its Gaussian profile. The theoretical analysis shows that a self-defocussing medium can behave as a negative power graded index (GRIN) lens with an intensity-dependent focal length at low incident intensities. This result was used to determine the upper limit of incident intensities where the PR medium can be described as quadratic with both real and imaginary components of the refractive index. It was shown that the imaginary component of the change in refractive index can have a self-focussing or defocussing effect independent of the real component of the refractive index and that the apparent self-focussing of a single Gaussian field in self-defocussing PR media is a result of the imaginary component of the intensity-dependent refractive index. This imaginary component can act with or against the self-focussing or self-defocussing action of the real component of the medium leading to anomalous observations in particular scenarios. Experimental results have also been presented, where appropriate, that show good agreement with the numerical considerations.

References

1. Y. Kivshar, Nat. Phys. **2**, 729 (2006)
2. A.W. Snyder, F. Ladouceur, Opt. Photon. News **10**, 35 (1999)
3. M. Segev, Opt. Quantum Electron. **30**, 503 (1998)
4. L.B. Kish, Phys. Lett. A **305**, 144 (2002)
5. M. Tokushima, H. Yamada, Y. Arakawa, Appl. Phys. Lett. **84**, 4298 (2004)
6. L. Risch, Mater. Sci. Eng. C **19**, 363 (2002)
7. J.T. Verdeyen, *Laser Electronics*, 3rd edn. (Prentice Hall, Englewood Cliffs, 1995)
8. A. Rausch, A. Kiessling, R. Kowarschik, Opt. Express **14**, 6207 (2006)
9. E. Jaatinen, M.W. Jones, Opt. Commun. **281**, 3201 (2008)
10. M.W. Jones, E. Jaatinen, Proc. SPIE **6801**, 68011P (2008)
11. D.A. Temple, R.S. Hathcock, C. Warde, J. Appl. Phys. **67**, 6667 (1990)
12. A.M. Glass, Opt. Eng. **17**, 470 (1978)
13. N. Barry, M.J. Damzen, J. Opt. Soc. Am. B **9**, 1488 (1992)
14. A. Yariv, *Quantum Electronics*, 3rd edn. (Wiley, New York, 1989)
15. H. Song, S.X. Dou, M. Chi, H. Gao, Y. Zhu, P. Ye, J. Opt. Soc. Am. B **15**, 1329 (1998)
16. M. Chi, S.X. Dou, P. Ye, Opt. Commun. **170**, 115 (1999)
17. M.W. Jones, E. Jaatinen, Opt. Mater. **31**, 122 (2008)
18. G.S. He, S.H. Liu, *Physics of Nonlinear Optics* (World Scientific, Singapore, 1999)
19. R.L. Sutherland, *Handbook of Nonlinear Optics*, 2 edn. (Marcel Dekker, New York, 2003)
20. M.W. Jones, E. Jaatinen, G. Michael, in *ACOLS* (2009), pp. 97–98
21. Y. Tomita, S. Matsushima, J. Opt. Soc. Am. B **14**, 2877 (1997)
22. D. Marcuse, S.E. Miller, Bell Syst. Tech. J. **43**, 1759 (1964)
23. A. Motes, J.J. Kim, Opt. Lett. **12**, 199 (1987)
24. G.A. Brost, R.A. Motes, J.R. Rotge, J. Opt. Soc. Am. B **5**, 1879 (1988)
25. H. Song, S.X. Dou, P. Ye, J. Appl. Phys. **88**, 6981 (2000)